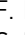## PAPER

Ambient and laboratory observations of organic ammonium salts in PM_1†

P. Schlag, [ID] ‡*[a] F. Rubach, [ID] §[a] T. F. Mentel,[a] D. Reimer, [ID] [a] F. Canonaco,[b] J. S. Henzing,[c] M. Moerman,[c] R. Otjes,[d] A. S. H. Prévôt,[b] F. Rohrer,[a] B. Rosati,¶[b] R. Tillmann,[a] E. Weingartner‖[b] and A. Kiendler-Scharr[a]

Ambient measurements of PM_1 aerosol chemical composition at Cabauw, the Netherlands, implicate higher ammonium concentrations than explained by the formation of inorganic ammonium salts. This additional particulate ammonium is called excess ammonium (e_{NH_4}). Height profiles over the Cabauw Experimental Site for Atmospheric Research (CESAR) tower, of combined ground based and airborne aerosol mass spectrometric (AMS) measurements on a Zeppelin airship show higher concentrations of e_{NH_4} at higher altitudes compared to the ground. Through flights across the Netherlands, the Zeppelin based measurements furthermore substantiate e_{NH_4} as a regional phenomenon in the planetary boundary layer. The excess ammonium correlates with mass spectral signatures of (di-)carboxylic acids, making a heterogeneous acid−base reaction the likely process of NH_3 uptake. We show that this excess ammonium was neutralized by the organic fraction forming particulate organic ammonium salts. We discuss the significance of such organic ammonium salts for atmospheric aerosols and suggest that NH_3 emission control will have benefits for particulate matter control beyond the reduction of inorganic ammonium salts.

[a]*Institute for Energy and Climate Research (IEK-8): Troposphere, Forschungszentrum Jülich, Jülich, Germany. E-mail: p.schlag@fz-juelich.de*

[b]*Laboratory of Atmospheric Chemistry, Paul Scherrer Institute (PSI), Villigen, Switzerland*

[c]*Netherlands Organisation for Applied Scientific Research (TNO), Utrecht, The Netherlands*

[d]*Energy Research Centre of the Netherlands (ECN), Petten, The Netherlands*

† Electronic supplementary information (ESI) available: Additional graphs and tables. See DOI: 10.1039/c7fd00027h

‡ Now at: Institute of Physics, University of Sao Paulo, SP, Brazil.

§ Now at: Max Planck Institute for Chemistry, Climate Geochemistry Department, Mainz, Germany.

¶ Now at: Department of Physics and Astronomy, Aarhus University, Aarhus C, Denmark.

‖ Now at: Institute for Aerosol and Sensor Technology, University of Applied Science Northwestern Switzerland.

Introduction

Ammonia (NH_3) is the most abundant volatile base in the atmosphere and plays a central role in the formation of particulate inorganic salts such as ammonium sulfate (($NH_4)_2SO_4$), ammonium nitrate (NH_4NO_3) and ammonium chloride (NH_4Cl) with the respective inorganic acid (sulfuric acid, nitric acid and hydrochloric acid). NH_3 sources are dominated by agricultural activities such as fertilizer use and livestock.[1] The aforementioned acid–base reactions are the dominant loss process for NH_3. Ambient concentrations of NH_3 depend strongly on the environment and can reach several ppm in the vicinity of large agricultural areas.[2] In recent years urban NH_3 concentrations have increased due to the use of selective catalytic reduction to remove nitrogen oxides from car emissions and stacks.[3,4] At the same time significant reductions have been achieved in the emissions of SO_2 in Europe,[5,6] which diminishes the role of sulfate aerosol but increases the availability of NH_3 to form other salts such as NH_4NO_3.[7] NH_4NO_3 is therefore observed to be the dominant inorganic PM_1 species in many parts of Europe.[8]

Dicarboxylic acids (DCA) are a prominent class of oxidation products of atmospheric VOC and have been observed in atmospheric aerosol in urban,[9–14] rural,[9,11] as well as marine environments.[15,16] Oxalic acid is often the most abundant DCA and has been shown to easily uptake NH_3 in laboratory conditions.[17,18] Previous field measurements and model studies suggest that ammonium salts of organic acids have to be accounted for in aerosol ion balances.[19–21] While the properties of inorganic ammonium salts are well characterized,[22] little is known about the physical properties of organic ammonium salts in particles. Uptake of ammonia on organic aerosol was suggested to change the hygroscopic properties[23] and volatility[18] of organic aerosol. It is also suspected to have an effect on the optical properties of aerosol, possibly accounting for brown carbon formation in aged organic aerosol (ref. 24 and references therein).

North-Western Europe is characterized as a polluted region affected by substantial agricultural emissions. The Cabauw Experimental Site for Atmospheric Research (CESAR) can be considered representative of rural North-Western Europe.[25] It has been shown recently that the aerosol concentration at this site regularly exceeds WHO limits.[26] The composition of PM_1 at this site is dominated by organics and NH_4NO_3.[26,27] Here we show observations from ground site and airborne measurements with a Time-of-Flight Aerosol Mass Spectrometer (ToF-AMS) from Cabauw, the Netherlands, indicating an efficient uptake of ammonia by the organic fraction in PM_1. The level of neutralization of organic acids is discussed in the context of laboratory reference measurements and an interpretation of the overall functionality of the organic responsible for ammonia uptake is provided. It is discussed that ammonia reduction strategies will reduce PM_1 exposure beyond the reduction of inorganic ammonium salts in this environment.

Experimental materials and methods

The CESAR Observatory is located in the western part of the Netherlands (51.971° N, 4.927° E) and provides measurement platforms at heights up to 213 m above

the surface. The site was established in 1972 and is used for long term atmospheric composition monitoring and surface-atmosphere exchange studies. Meteorological data and gaseous compounds, including greenhouse gases, are monitored routinely at the tower.[25,28,29]

A ToF-AMS[30–32] was used to measure PM_1 non-refractory chemical composition, including the organic fraction (Org), ammonium (NH_4), nitrate (NO_3), sulfate (SO_4), and chloride (Chl), at the CESAR tower from May 12th to July 17th 2012 with a time resolution of 7 minutes. The ToF-AMS was sampling at ambient RH from an aerosol inlet installed at a 5 m inlet height, keeping a laminar flow regime. The total residence time of the sample air in the inlet was approximately 20 seconds. The contribution to the CO_2^+ signal from gas phase CO_2 was subtracted by using data from periodically performed measurements with a HEPA filter inline the AMS inlet. The CO_2^+ signal derived from the particulate organic fraction is referred to as Org-CO_2.

During mass calibrations (see below), using concentrations of ammonium nitrate of up to 30 µg m^{-3}, no significant CO_2^+ signals were observed for all AMS instruments reported here. Therefore, a potential CO_2^+ interference caused by ammonium nitrate as shown by ref. 33 can be excluded. Equivalent black carbon (eBC) in PM_{10} was measured in parallel with a Multi-Angle Absorption Photometer (MAAP, Thermo Scientific Model 5012) at 60 m height. Although the MAAP has no size selective inlet beside the PM_{10} heads, it can be assumed that eBC-containing aerosols generally fall into the submicron size range.[34] Thus, eBC concentrations obtained from the MAAP can be added to the AMS measured NR-PM_1 mass for completeness.

The vertical and horizontal extent of the local ground site measurements was explored in two flights of the Zeppelin NT on May 21st and May 22nd during the Pan-European gas-aerosols-climate interaction study (PEGASOS) campaign. The Zeppelin NT is a semi-rigid airship of 75 m length and a maximum hull diameter of 14 m. Different to fast moving aircraft often used to characterize chemical processes at different altitudes, the Zeppelin is able to operate at low velocities throughout the lowest kilometer of the atmosphere.[35] Thus it is an ideal platform for performing height profiles over a confined area. Instruments measuring the highly reactive OH and HO_2 radicals, and the total reactivity of OH radicals, were permanently mounted at the platform on top of the airship.[36] All other instruments described here were installed inside the cabin, sampling ambient air with inlet lines either from the nose-boom at the tip of the gondola, from below the bottom hatch, or from a window in the front door of the gondola.

For the two flights on May 21st and May 22nd the Zeppelin NT cabin configuration was the so called SOA layout. It was equipped with a ToF-AMS trimmed to save weight (hereafter termed ZAMS, Aerodyne Inc[35]), an aethalometer for eBC, a CPC and a SMPS for particle number concentration and particle size measurements, as well as instruments to measure gas phase tracers NO, NO_2, O_3, CO and VOC.[35–38] A comprehensive description of the ZAMS, including its mechanical and electronic adaption to on board conditions on the Zeppelin NT is given elsewhere.[35] Note that the ZAMS was operated with a pressure dependent inlet[39] to compensate for ambient pressure changes during flights. The flight on May 21st was conducted from Rotterdam Airport to a forest in the Putten municipality, Gelderland, Netherlands, and included measurements at 3 different heights at Putten, later at Wageningen, Netherlands, and finally Cabauw, before

the Zeppelin flew back to the airport. The altitude changes were performed with ascend or descend rates of around 3 m s^{-1}. Height profile measurements at the CESAR tower onboard the Zeppelin were performed at 3 flight levels between 50 and 375 m, each probed for 5–6 min. The ZAMS was operated with a time resolution of 30 seconds, thus providing at least 9 data points at each height. We included one data point at approximately 150 m in our vertical profiles, which was acquired during a height transition. The overall flight duration over Cabauw was 57 minutes between 12:47 and 13:44 local time.[35] The second flight on May 22nd did not include height profiles but represents a transect flight from Rotterdam Airport to Cabauw, from there *via* Rotterdam to the North Sea and back to the airport. Over the sea, the Zeppelin switched to a higher altitude and the flight back to the airport was continued at a higher altitude than the flight to the sea. Map overviews of the flight tracks are shown in Fig. S3 and S4.†

Mass concentrations from the ToF-AMS were determined using a composition dependent collection efficiency (CDCE) correction.[40] For the ZAMS data set a CE of 1 was applied based on statistical analysis of mass concentrations derived from the SMPS measurements and from the combined data of the aethalometer and ZAMS.[37] The ionization efficiency (IE) of nitrate was calibrated for the ToF-AMS at least weekly, using the mass based method described in ref. 31 while the so-called brute force single particle method (for AMS single particle measurements see ref. 41) was applied for the calibration of the ZAMS. The relative ionization efficiency of NH$_4$ (RIE$_{NH_4}$) was determined directly from each IE calibration and resulted in an averaged value of 4.24 $\pm$ 0.14 for the ground based measurements. A RIE$_{NH_4}$ of 4.00 was calculated from an IE calibration of the ZAMS directly before the flights investigated here. RIEs for particulate organics, sulfate, and chloride (1.4, 1.2, and 1.3, respectively) were taken from the literature.[17,42,43]

Elemental ratios such as O/C, H/C, N/C of high resolution mass spectra were determined by implementing the correction factors established by ref. 44 and 45. As it was not possible to fit the CHO$^+$ ion within the ZAMS data due to high interferences with the ^{15}N^{14}N$^+$ signal, the elemental analysis method given by ref. 46 could not be used here. Consequently, ToF-AMS ground based data was analyzed similarly to ensure comparability of the two datasets.

In order to explore the vertical distribution of individual sources contributing to the organic aerosol, common organic factor profiles had to be established for the ground based ToF-AMS and the airborne ZAMS data. Accounting for the amount of data available (11 582 data points with 7 min time resolution for ToF-AMS and 33 data points with 0.5 min time resolution for ZAMS) the following approach was chosen for combined factor analysis of the organic aerosol component. For the ground based AMS data, factor analysis of the organic fraction of the aerosol was performed using Positive Matrix Factorization (PMF) analysis,[47,48] applying the PMF2-solver software PMF Evaluation Tool (PET[49]), version 2.06 beta, within Igor Pro 6.2.3. PMF is a bilinear model and assumes that the original data set, containing variable mass spectra over time, is a linear combination of a given number of factors, each with a constant mass spectrum and varying contribution over time. The strategy to perform factor analysis and explore PMF solutions for the ground base data was taken from ref. 50 and has been successfully used in ambient studies apportioning the measured organic mass spectra in terms of source/process-related components. The organic fraction measured by the ZAMS was investigated *via* the ME-2 solver version 4.8,[51]

implemented within the Igor Pro based Source Finder (SoFi[52]). With the ME-2 solver it is possible to introduce *a priori* mass spectral information and hence to reduce the rotational ambiguity, *i.e.*, similar PMF results with the same goodness of fit, of PMF solutions.[53] In this work, PMF factors derived from exploration of the ground base data set as described above were used as constraints without any freedom given to the model (*a*-value = 0, see ref. 52) for PMF calculations of the ZAMS data set.

An important aerosol property is the acidity, *i.e.* the concentration of H^+ ions in the aqueous phase. When the majority of inorganic species (>95%) are accounted for, alkaline particles can be distinguished from acidic particles with good reliability by the molar ratio of cations and anions.[54] The sensitivity of the AMS for salts containing alkali metals or alkaline earth metal cations is very low due to the 600 °C oven temperature in the AMS and the high temperature of evaporation of these salts. At the CESAR tower measurements with a Monitor for Aerosol and Gases (MARGA, Applikon Analytical BV, see ref. 55) were performed to determine PM_1 ion composition. These show only low concentrations of Mg^{2+}, Na^+, K^+, and Ca^{2+} (average sum over the entire campaign: 0.08 µg m^{-3}). Thus the main inorganic aerosol anions NO_3^-, SO_4^{2-}, and Cl^- and the cation NH_4^+ are used in the following to determine the ion balance.

Because of charge neutrality a deficit of NH_4^+ required to fully neutralize anions to NH_4NO_3, $(NH_4)_2SO_4$, and NH_4Cl is assumed to be balanced by a respective amount of H^+ ions. On the contrary, a higher abundance of NH_4^+ than is needed for neutralization of the particulate anions is considered as excess NH_4 (e_{NH_4}). As discussed below in this work we will assume that e_{NH_4} is neutralized by organic acids. The mass concentration of e_{NH_4} can be calculated from eqn (1), where MW_{NH_4} represents the molecular weight of NH_4 and n_i is the molar concentration of species i in the aerosol.

$$e_{NH_4} = MW_{NH_4} \times [n_{NH_4} - (n_{NO_3} + 2 \times n_{SO_4} + n_{Cl})] \qquad (1)$$

Only the inorganic nitrate (In_{NO_3}) is used for the ion balance, since organic nitrates are already neutralized by their organic fragments. In this work organic nitrate was determined based on the relative abundance of NO_2^+/NO^+ ions as described in ref. 56 and 57. The NO_2^+/NO^+ ratio for pure inorganic nitrate was determined from the respective ratio of the weekly calibrations using pure NH_4NO_3 and found to be relatively constant for the ToF-AMS during the entire campaign (0.39 ± 0.02). The ZAMS showed higher values, on average 0.65 and higher variations between 0.6 and 0.78. The highest value of 0.78 was determined on May 20th, *i.e.* closest to the flights reported here. Nevertheless, the campaign average value for pure ammonium nitrate (0.65) was applied for the calculation of the organic and inorganic nitrate fractions, as it reduces the uncertainty of a single calibration and provides a lower limit of OrgNO$_3$ and thus of e_{NH_4} concentration (see eqn (1)). An upper limit of the e_{NH_4} concentration was calculated using the maximum NO_2^+/NO^+ ratio of 0.78. The results of this are reported as maximum e_{NH_4} below.

The limit of detection of e_{NH_4} was derived in laboratory experiments. For this purpose, e_{NH_4} was determined for pure NH_4NO_3 and $(NH_4)_2SO_4$ particles as function of inorganic mass concentration. It was shown that at mass concentrations larger than 10 times the detection limit of NH_4, a reliable ion balance and

thus e_{NH_4} determination is provided. The detection limit of NH_4 was determined in NH_4NO_3 calibrations during the field campaigns for the ToF-AMS and ZAMS instruments and found to be 0.06 µg m^{-3} and 0.01 µg m^{-3}, respectively. For all but 16 data points (out of 11 582) of ToF-AMS data shown in this work, NH_4 concentrations were above this value. The ZAMS measured NH_4 concentrations were above 1 µg m^{-3} throughout the flights reported here. We therefore consider the full data set as applicable to e_{NH_4} analysis.

We propose that the anions of organic acids counterbalance the excess ammonium. Therefore, laboratory experiments were performed to test the hypothesis that uptake of NH_3 *via* acid–base reactions on condensed phase organic acids can lead to e_{NH_4}. For that, dry and wet monodisperse particles of pure organic acids were generated and directed to a flow tube made of borosilicate glass. There, the aerosols were exposed either to a pure or to a NH_3 containing N_2 gas flow for a total of ~ six minutes residence time. The NH_3 concentration during the uptake experiments was kept to around 10 ppb as monitored by a Cavity Ring-Down Spectrometer (CRDS, Picarro Model G2103). The aerosol chemical composition was measured by a Quadrupole Aerosol Mass Spectrometer (QAMS). The particle concentrations were adjusted so that the molar concentrations of particulate acid groups were in the same range as the molar concentrations of the gaseous NH_3 in the flow tube. This was done to ensure a potential complete neutralization of the acid groups by ammonia at atmospherically relevant concentrations of both reagents. Like for the ambient AMS data gas phase background, measurements were done for all experiments by acquiring data with a particle filter in front of the QAMS inlet to ensure that signals on *e.g.* m/z 44 solely derived from sampled particles. Note that carboxylic acid groups are considered to be detected as equal amounts of CO^+ and CO_2^+ ions by the AMS.[45] This is due to the fact that even in high mass resolution (ambient) AMS measurements the N_2^+ signal on m/z 28 is too high, so that the signal of the CO^+ ion can usually not be determined directly from the mass spectra. As summarized

Table 1 Overview of the results from lab experiments on the uptake of NH_3 on pure organic substances: organic acids (black), ascorbic acid (blue), and sugars (green). The relative humidities were in the range of 75–85%, if not otherwise specified

Substance	f_{44}[a]	Molar ratio NH_3/acid	e_{NH_4} [µg m^{-3}]	Yield$_{neutr}$ [%]	Penetration depth [nm]
Adipic acid	0.13	13 : 1	0.05	1	1
Succinic acid	0.18	2 : 1	0.10	2	1
Glutaric acid	0.11	2 : 1	0.3	4	2
Citric acid	0.24	9 : 1	0.56	19	9
DL-Malic acid	0.21	8 : 1	0.96	21	11
L-Tartaric acid; RH > 75%	0.24	2 : 1	1.6	24	12
L-Tartaric acid; RH > 75%	0.21	7 : 1	2.0	36	19
L-Tartaric acid; RH > 75%	0.22	17 : 1	3.1	36	19
L-Tartaric acid; RH = 30%	0.22	6 : 1	6.0	31	16
Ascorbic acid	0.19	4 : 1	0.9	25	13
Glucose	0.05	—	—	—	—
Sucrose	0.03	—	—	—	—

[a] Determined directly from QAMS data during the respective experiment.

in Table 1 five dicarboxylic acids, a tricarboxylic (citric acid) and an acid with no carboxylic acid groups but an acidic OH group (ascorbic acid) were investigated. In addition, sucrose and glucose were studied as reference substances for which no NH_3 uptake was expected.

Results

The bottom graph in Fig. 1 shows the temporal evolution of PM_1 mass concentrations (stacked) of equivalent black carbon (eBC, black), organics (Org, green), nitrate (NO_3, blue), sulfate (SO_4, red), ammonium (NH_4, orange), and chloride (Chl, pink) as measured by the MAAP and AMS, from May to July 2012. The average total mass concentration was 6.40 μg m^{-3}. NO_3 and organics were the dominant species throughout the whole campaign, which was also observed in previous campaigns at the CESAR tower.[26,27] Several periods with high aerosol mass loadings were observed. Between May 20th and May 23rd in the afternoon, the total mass concentration increased continuously up to 35.0 μg m^{-3} with an average of 19.0 μg m^{-3}. During this time, northerly and north westerly wind directions prevailed and NO_3 and organics were still the dominant species.

The top graph of Fig. 1 displays the mass concentration of excess ammonium (e_{NH_4}, brown). Peak values of up to 0.5 μg m^{-3} were determined during the indicated high mass periods including the time at which the Zeppelin flew over the CESAR tower (black vertical line) and where height profiles shown in this work were acquired. An average e_{NH_4} concentration of 0.05 μg m^{-3} was determined, resulting in average mass fractions of 5% and 1% with respect to total NH_4 and total aerosol mass. Periods with negative values of e_{NH_4}, indicating acidic aerosols,
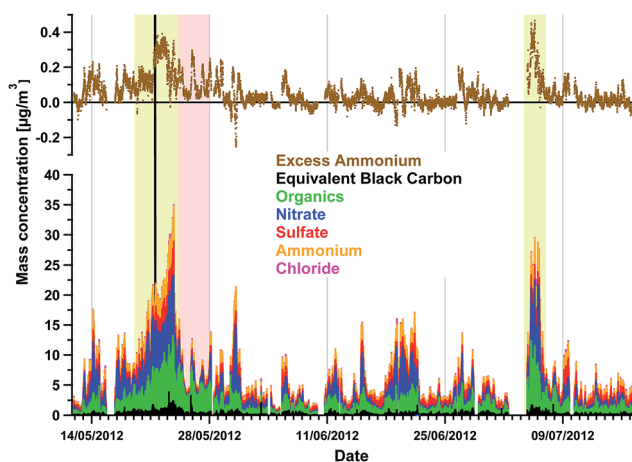

Fig. 1 Aerosol composition from ground based measurements. Top panel: Excess ammonium mass concentrations calculated according to eqn (1). Bottom panel: Stacked time series of mass concentrations of aerosol components. High mass periods are indicated by light green backgrounds. The time period with easterly wind directions and high relative organic contribution is highlighted in red. The black vertical line marks the Zeppelin flight at the CESAR tower on May 21st 2012.
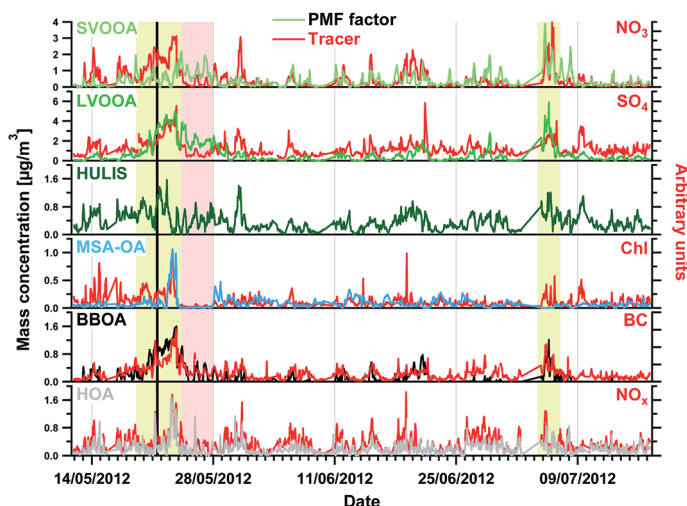
Fig. 2 Time series of PMF factors from AMS ground based data and tracers. High mass periods are indicated by light green backgrounds. The time period with an easterly wind direction and high organic contribution is highlighted in red. The black line marks the Zeppelin flight at the CESAR tower on May 21st 2012. The bottom of all tracer axes is set to zero.

are rarely observed and are of very short duration (maximum 6 hours of continuous significant acidity).

Statistical analysis of organic aerosols – ground data

The unconstrained PMF analysis of the AMS ground based organic fraction obtained six factors (FPEAK = 0). Their time series and mass spectra are displayed in Fig. 2 and S1,† respectively. Fig. 2 contains also the time series of important external tracers, which are commonly used to identify specific organic factors.[50] An overview of the correlation coefficients between the most important tracers and the six factors is given in Table S1.† Besides the primary organic aerosol (POA) factors HOA (hydrocarbon-like organic aerosol) and BBOA (biomass burning factor), three more oxidized organic profiles were found with increasing O/C ratios: a semi-volatile oxygenated organic aerosol (SVOOA), a low-volatile OOA (LVOOA) and a HULIS factor (see below). All SOA factors (SVOOA, LVOOA, and HULIS) together contribute 77% to the total organic fraction. The sixth factor was attributed to methanesulfonic acid (CH_3SO_3H, MSA), and thus is called MSA-OA. The HOA, BBOA, SVOOA and LVOOA factors have been commonly seen in a number of AMS campaigns (*e.g.* ref. 50), including campaigns at the CESAR tower.[17,58] The MSA-OA factor showed only a few high mass concentration events, *e.g.* from 23rd to 24th May. That is why this factor contributes little (4%) to total organics over the entire campaign. This event is also accompanied by a high mass peak of particulate chloride. The high fraction of organic sulfate ions to the MSA-OA profile attributes this factor to marine sources. This factor class was not only observed in marine environments,[59,60] but also in the continental megacity of Paris.[61]

The so called HULIS factor showed the highest O/C ratio of all factors, mainly resulting from a higher contribution of the CO_2^+ ion than, *e.g.*, the LVOOA factor. The HULIS factor class was first observed by the authors of ref. 62 in previous AMS campaigns at the CESAR tower in May 2008 and March 2009. These findings were confirmed for 2008 by a re-analysis using the ME-2 solver, published in ref. 58. The identification and characterization of this factor class was achieved by comparison with data from an ion-exchange chromatographic method for the direct quantification of humic-like substances (HULIS) and from water-soluble organic carbon (WSOC) analyzed offline on a set of filters collected in parallel.[63] Such measurements were not available in the campaign reported here. A high correlation was found between the HULIS profile observed in this study and the reference HULIS spectra ($R^2 = 0.91$ and 0.88, compared to ref. 58 and 62,
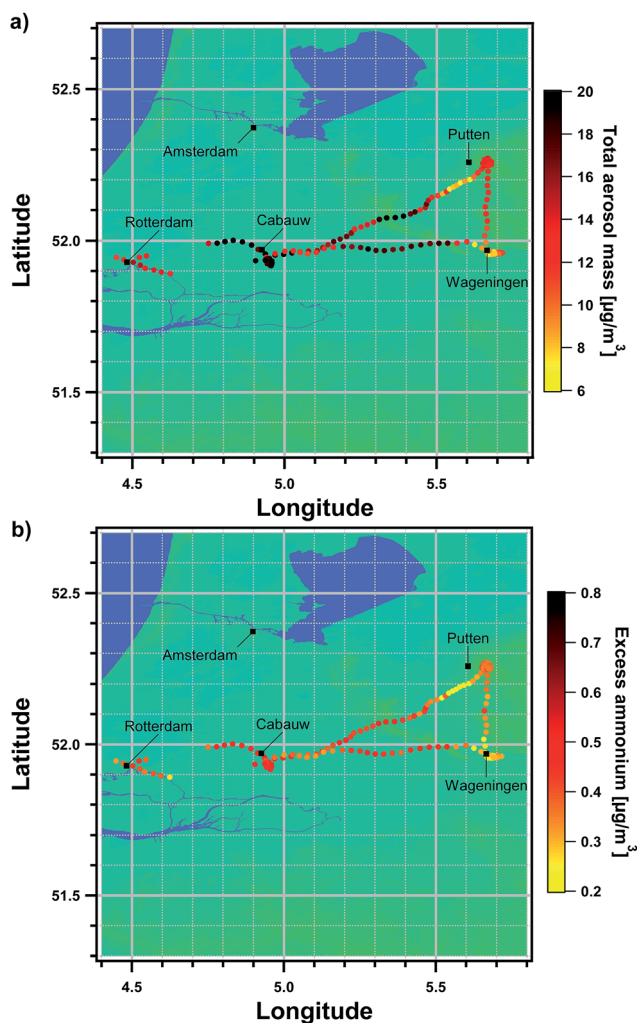

Fig. 3 Zeppelin flight tracks on May 21st, color coded with the (a) total PM$_1$ mass concentrations and (b) the e$_{NH_4}$ concentration.

respectively). Similar to the results reported there, no significant time series correlation was found for the HULIS factor in 2012.

Zeppelin data

Fig. 3a and b show the Zeppelin flight track from May 21st, color coded by the total PM$_1$ mass concentrations and the excess ammonium concentration. Similar to the ToF-AMS data, organics and nitrate are found to be the dominant species over the entire flight. The air above Wageningen contained the lowest nitrate concentrations, resulting in an increase of the organic fraction at that location. As for the AMS data set at the CESAR tower, high e_{NH_4} abundances occurred at times with high total aerosol masses, which are mainly observed around Cabauw, but also between Cabauw and the two cities, Putten and Wageningen. The highest values of e_{NH_4} were determined at Cabauw, which reach up to 0.53 µg m^{-3} and represent 1% and 7% of the total particle mass and total NH$_4$ concentration, respectively. A rather low total mass and e_{NH_4} were determined over the two cities. As mentioned in the Experimental section, a lower and an upper limit of the inorganic nitrate fraction was used for the ion balance to determine excess ammonium. Concentrations for lower limits of e_{NH_4} in this analysis derived from the used campaign average of the NO$_2^+$/NO$^+$ ratio. In Fig. 3 we show the lower limit of e_{NH_4}, for comparison the upper limit of e_{NH_4} is shown in Fig. S3.† Fig. S3† in the Supplementary Information also displays the respective flight tracks for e_{NH_4} during the transect flight on May 22nd with higher concentrations of up to 0.67 µg m^{-3} at low altitudes (below 200 m) over the sea, 6 km past the shore.
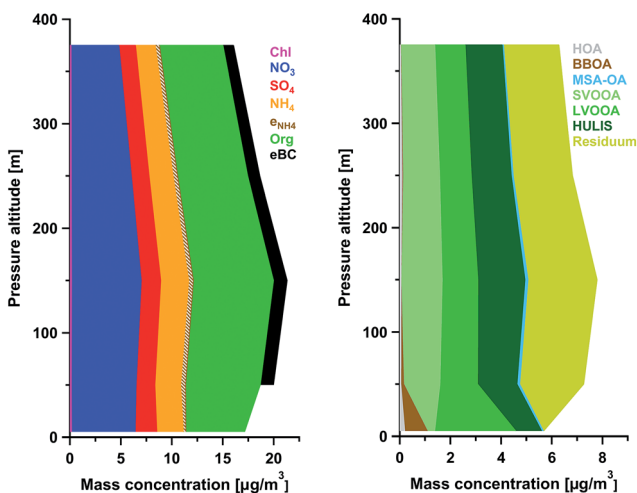

Fig. 4 Height profiles of individual species from AMS measurements (left) and vertical distribution of organic factors and residuals (right). The concentrations at 5 m height were measured by the ground based ToF-AMS. Note that excess ammonium is displayed here as part of total ammonium. Height profiles of organic factors were obtained using the ME-2 solver on both AMS data sets. All factors, as found from unconstrained PMF explorations of the ground based organic fraction as described in the Experimental section, were fully constrained (a-value = 0). Note also that the MAAP at the CESAR tower was sampling at 60 m height, thus only eBC data from the Zeppelin is shown.

Both ZAMS and ground based AMS data sets were combined to height profiles shown in Fig. 4.

Statistical analysis of organic aerosols – height profiles during Zeppelin flights

As the number of data points from the height profiles acquired by the ZAMS (33 points) is not sufficient to perform unconstrained PMF explorations and regression analyses with tracers, a calculation using the ME-2 solver with fully constrained factors was done using the six PMF factors found from the ToF-AMS organic fraction as described above. This procedure assumes that organic factors observed at the ground are present at higher altitudes as well. As a consequence, this approach will assign organic aerosol that does not match any of the factors found at the ground to the residuum. Also chemical aging of organic aerosol that results in a change in its mass spectral pattern will also be considered as a residual signal in this approach. To ensure that the ME-2 solver is consistent with the unconstrained PMF solution, we also performed constrained PMF analysis of the ToF-AMS data using the ME-2 solver. There, the residuals were consistent with the results from unconstrained PMF.

Fig. 4, right panel, shows the height profiles of mass concentrations of each organic factor, together with the total residuals of the respective ME-2 exploration. As expected, the residuum at the ground is negligible, while from the ZAMS data high residuals corresponding to 2.3 µg m^{-3}, or 33% of organics on average, were seen. The mass spectrum of this residuum contains important diagnostic information and is displayed in Fig. 5. It shows a high fraction of nitrogen containing ions by means of nitrogen- and nitrate-containing ions, together with a very high nitrogen-to-carbon (N/C) ratio of 0.11 compared to the other factors, where N/C ratios do not exceed 0.02. Most of these ions were not detected in the ToF-AMS data set at 5 m and therefore not fitted. Important exceptions are two ions of m/z 58, namely $C_4H_{10}^+$ and $C_3H_8N^+$, which were also fitted for the ground based data but showed a much lower signal than seen in the ZAMS data. Both ions together comprised 40% of the ZAMS residual signal. $C_3H_8N^+$ is considered as
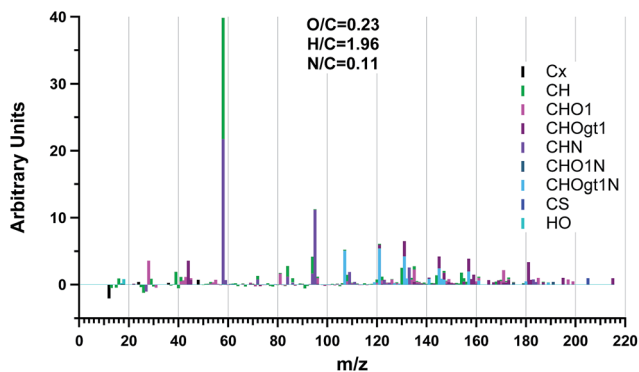

Fig. 5 Mass spectrum of the residuum using the ME-2 solver on the ZAMS data set for the height profile at the CESAR tower on May 21st, as shown in Fig. 4, right graph, and as described in the text. The HR mass peaks are stacked at each unit mass m/z and colored by their chemical family (gt1 = greater than 1).

a tracer for reduced nitrogen compounds such as amines.[50,64] These observations indicate that aerosols at higher altitudes contain a much larger fraction of particulate amines and/or organonitrates, which confirms the findings of higher concentrations of OrgNO$_3$ and e_{NH_4} as determined above.

Laboratory experiments on NH$_3$ uptake

The laboratory experiments on the NH$_3$ uptake on pure organic particles as described in the Experimental section show that (dicarboxylic) acids are indeed capable of binding gaseous ammonia *via* an acid–base reaction to become particulate ammonium in the absence of inorganic anions (Table 1). The yield of neutralization (Yield$_{neutr}$) represents the molar fraction of organic acid groups, which is neutralized by measured excess ammonium, assuming that particles consist of the pure respective substance free of significant contamination. Note that for none of the substances studied was full neutralization achieved on the time scale of the experiment ($\sim$ 6 minutes). This is likely due to the mixed influence of particle morphology of single compound organic acid particles and particle size. The relative humidity within the experimental setup (usually between 75% and 85%) did not always exceed the deliquescence points of those compounds, especially in cases of succinic, glutaric and adipic acid. Hence the aerosol consisted probably of more solid particles which may inhibit the uptake and transport of NH$_3$ within the particle volume. Taking this assumption into account, the depth of a layer was calculated (from hereon called penetration depth), within which full neutralization of the organic di-acids by ammonia was theoretically achieved. Table 1 provides the results for each compound. As can be seen, these depths range between 1 and 20 nm for particle diameters of 280 nm.

As expected the non-acidic test substances glucose and sucrose do not show any uptake of NH$_3$ at all even under very high ammonia levels of up to 61 ppb. Note that compared to the investigated organic acids, only low f_{44} signals were determined in the QAMS for both substances as seen in Table 1. For ascorbic acid however, a behavior similar to (di-)carboxylic acids was observed, namely a significant uptake of ammonia and a relatively high f_{44} due to the intra-molecular ester group which means that the signal on m/z 44 cannot be directly taken as a proxy for the amount of carboxylic acid groups within ambient particles. It can be concluded that organic acids take up NH$_3$ from the gas phase to form particulate organic salts. The observed excess ammonium provides a lower limit for quantifying organic acids in aerosols, as at least on the time scale of the reported laboratory experiments, no full neutralization was achieved as shown by penetration depths in the range of a few nm. For analysis we applied the assumption that carboxylic acids equally fragment into CO$^+$ and CO$_2^+$ in the AMS. Therefore, another uncertainty arises if specific organic acids show a deviating fragmentation ratio. In addition, carboxylic acids can undergo intra- or inter-molecular reactions, forming anhydrides,[65,66] which may still contribute significantly to the AMS CO$_2^+$ signal but will not react with NH$_3$ in an acid base reaction.

Discussion

The results of both the ground based and airborne AMS data sets show high e_{NH_4} concentrations especially during periods with high total aerosol abundances,

where e_{NH_4} represents up to 5% of total NH_4 concentrations at ground and 7% at higher altitudes above the CESAR tower. Those findings were observed as well in previous AMS campaigns at the CESAR site in May 2008, reported in ref. 27, with a contribution of 4% to total mass and 2% in November 2011.[67] For the latter campaign, the time series of e_{NH_4} is shown in Fig. S2.† Therefore, e_{NH_4}, probably bound to carboxylic groups (organic acids), contributes significantly to aerosol mass, and thus influences air quality at the rural site of Cabauw. In addition, as e_{NH_4} was determined at several other locations in the Netherlands during the two Zeppelin flights reported here and is clearly a regional phenomenon.

Regression analyses of e_{NH_4} with several aerosol and gas phase tracers are summarized in Table S2† and show good correlation with the particulate organic CO_2 signal which is considered an indicator for organic acids in the AMS (ref. 68 and references therein). Scatter plots between the molar concentrations of e_{NH_4} ($n_{e_{NH_4}}$) and Org-CO_2 (n_{Org-CO_2}) for the entire ToF-AMS campaign and the two Zeppelin flights are displayed in Fig. 6. Assuming that each available carboxylic acid group combines with an e_{NH_4} molecule *via* an acid–base reaction, a ratio of $n_{e_{NH_4}}$ to n_{Org-CO_2} of 2 would be expected when carboxylic acid groups fragment within the AMS to equal amounts of CO^+ and CO_2^+ ions. The Org-CO_2 concentrations shown here consider the signal of CO_2^+ only. For the ground based observations, a slope of 0.71 is determined for the whole measurement period of two months. However, using only ground based ToF-AMS data acquired during both flights on May 21st and May 22nd resulted in a much higher slope of 1.30 ($R^2 = 0.38$) compared to the campaign average. This verifies the higher slope from the ZAMS data of 1.61 as averaged over the two entire flights. The correlation of the maximum ZAMS $n_{e_{NH_4}}$ to n_{Org-CO_2} by the use of the single calibration NO_2^+/NO^+ ratio in determining ZAMS organic nitrate mass concentration would result in a slope of 2.87 ($R^2 = 0.75$), which is higher than the theoretical value of 2. Although the slopes of both correlations do not agree with the theoretical slope, the high correlation coefficients indicate that carboxylic acid groups explain at least part of the excess NH_4 uptake.
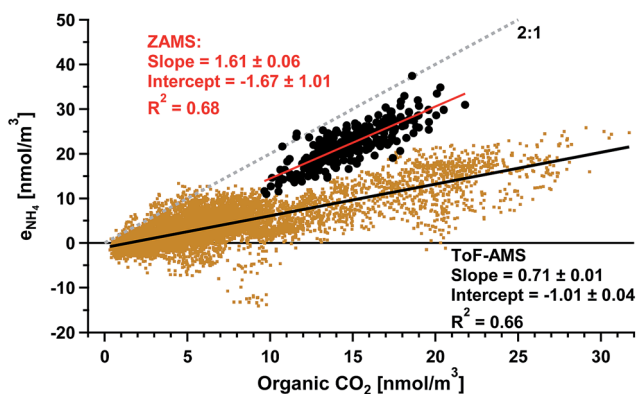
Fig. 6 Correlation plots of $n_{e_{NH_4}}$ and n_{Org-CO_2} for the ToF-AMS (brown) and ZAMS (black) data sets. The grey, dashed line represents the theoretical 2 : 1 regression line in case of full neutralization of e_{NH_4} by organic acid groups (see text). The red and black lines are derived from the regression analyses from the ZAMS (combined entire flights on May 21st and May 22nd) and the ToF-AMS data (whole campaign), respectively.

Reasons for a lower slope as observed for the ground based and airborne AMS data may be (a) a kinetically limited uptake of ammonia, (b) the presence of organic acids, with acid strengths lower than the one of NH_4^+ ($pK_s(NH_4^+) = 9.26$)[69] which are not able to bind ammonia *via* an acid–base reaction, but still contribute to the Org-CO_2 signal, and (c) the contribution of functional groups other than organic acid groups to CO_2^+ ions. However, in the latter case, a good correlation between $n_{e_{NH_4}}$ and n_{Org-CO_2} would imply that particulate molecules with such functional groups have similar time series, or in other words, a similar source like particulate molecules with carboxylic acid groups, or that these molecules are even identical. A potential low ambient NH_3 concentration, which would limit the NH_3 uptake, would only explain the varying $n_{e_{NH_4}}$ concentration, but not the good correlation to organic acid groups. In other words, the theory of the acid–base reaction would not be refuted. The slightly higher slope derived from ZAMS data is considered to be due to a more aged aerosol fraction found at higher altitudes, resulting in a larger amount of acids and/or acids with higher pK_s values strong enough to undergo an acid–base reaction with gaseous ammonia.

To gain more information about the nature of the organic fraction, which takes up excess ammonium, correlation analyses between e_{NH_4} and the organic PMF factors for the ambient AMS data were performed. The results of this analysis are shown in Table S2.† For the ToF-AMS data, e_{NH_4} showed the highest correlation with the LVOOA factor ($R^2 = 0.66$) and a moderate correlation with the BBOA factor ($R^2 = 0.49$), averaged over the entire campaign. These results are compatible with the relatively high contributions of CO_2^+ to these profiles, expressing a significant amount of carboxylic acid groups within the factors. An exception to this systematic relationship was found by the low correlation between the time series of e_{NH_4} and the HULIS factor ($R^2 = 0.36$), although its mass spectral profile was highly dominated by CO_2^+.

As mentioned before, the limited number of data points of the ZAMS height profile data (33 points) does not allow for proper regression analyses. However, for fully constrained PMF explorations using the ZAMS data of the entire flights of May 21st and May 22nd in separate approaches (consisting of 187 and 85 data points, respectively), good correlations were seen between ZAMS-e_{NH_4} and the respective HULIS factor time series, which is considered as not only local but regional background aerosol, with coefficients of $R^2 = 0.54$ and $R^2 = 0.50$, respectively. Such correlations were not seen between for LVOOA factor neither with the ZAMS-e_{NH_4}, nor with the maximum ZAMS-e_{NH_4} time series. Note that all factors were constrained using the PMF mass spectra obtained from the two month measurements at the CESAR tower. It was found before that HULIS can be considered a regional background factor at the site, implying that the mass spectrum and contribution to organics is stable over time. This mass spectral invariance may be less pronounced for LVOOA, which shows a stronger dependence on wind direction. For the flight on May 21st a slight correlation of the ZAMS-e_{NH_4} was seen with the residuum of the PMF examination ($R^2 = 0.44$), consistent with the fact that the residual also in this case mainly consists of amines and organonitrates (see Fig. S5†). The respective correlation coefficient for the whole flight on May 22nd is rather low ($R^2 = 0.19$), but regarding only the data points during the flight over the sea, where the highest e_{NH_4} concentrations on this flight were seen, a much better agreement was observed ($R^2 = 0.60$). HULIS is characterized by a poly-acidity, similar to fulvic acid, confirming that the agreement with e_{NH_4} is due to acid–base reactions of ammonia with organic

acids at least at higher altitudes. On the other hand, HULIS can also have a low aromaticity, higher H/C molar ratios, and a weaker acidic nature than fulvic acid (ref. 70 and references therein). This may explain the apparent disagreement between its acidity and the low correlation with e_{NH_4} as determined by the ToF-AMS on ground.

Knowing the fractional abundance of CO_2^+ of the LVOOA and HULIS factor profiles, the time series of the LVOOA-CO_2 and HULIS-CO_2 molar concentrations were determined and correlated to the molar concentration of excess ammonium in Fig. 7a and b, respectively. The slope of the regression line in Fig. 7a of 0.90 is still lower than the expected ratio $n_{e_{NH_4}}$ to $n_{LVOOA-CO_2}$ of 2, but higher than the slope achieved by the correlation of e_{NH_4} and the total Org-CO_2 concentration. As low volatile organic compounds, represented by the LVOOA factor, are considered to contain a high amount of (di-)carboxylic acids, it can be taken as additional confirmation that these compounds are most likely one of the main class of molecules responsible for ammonia uptake, forming particulate ammonium *via* acid–base reaction.

The slope of 1.9 between the ZAMS $n_{e_{NH_4}}$ to $n_{HULIS-CO_2}$ (Fig. 7b) achieved from both Zeppelin flights combined (when flight data is separated: 2.1 and 1.6 on May 21st
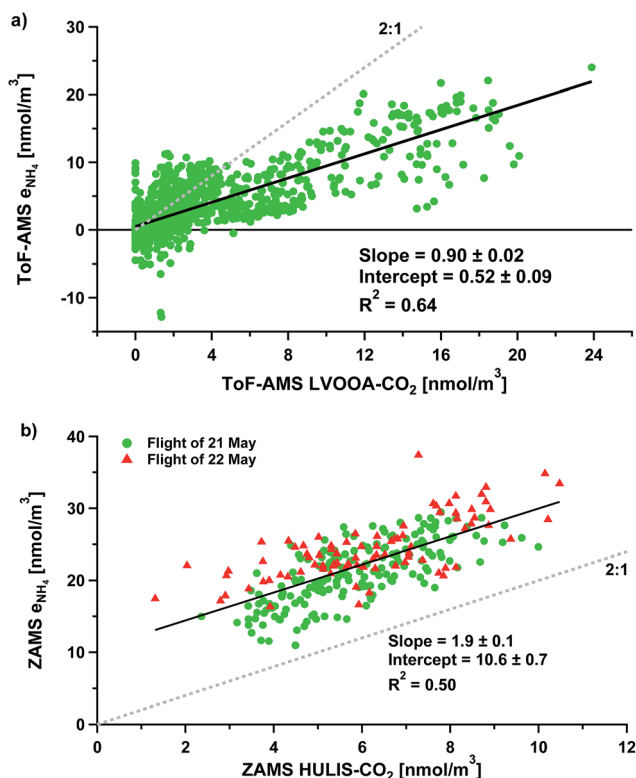

Fig. 7 Correlation plots of $n_{e_{NH_4}}$ and (a) $n_{LVOOA-CO_2}$ and (b) $n_{HULIS-CO_2}$ found for the ToF-AMS data set and for both entire Zeppelin flights combined, respectively. Note that by definition, PMF factors only consist of positive data values. Similar to Fig. 6, the grey, dashed lines represent the theoretical 2 : 1 regression line in the case of full neutralization of e_{NH_4} by respective organic acid groups (see text).

and May 22nd, respectively) however, fits to the expected ratio, but the intercept is high as well, pointing to a substantial other contribution to e_{NH_4}. The regression results using the maximum e_{NH_4} are shown in Fig. S6† and give an even higher slope and only a slightly lower intercept. Taking LVOOA into account, the slope between the ZAMS-$n_{e_{NH_4}}$ and the sum of the molar CO_2^+ concentrations from both highly oxidized SOA factors, LVOOA and HULIS, reaches a value of 1.5 ($R^2 = 0.59$) with a still substantial intercept of 5.2. But separate analyses of the two flights give a slope of 1.9 ($R^2 = 0.63$) with a low intercept of 0.65 in the case of the flight on May 21st. This may imply that the NH_3 uptake cannot be exclusively explained by the carboxylic groups of the HULIS factor, but combined with the respective acid groups of both SOA factors. For the second flight on May 22nd the same calculation leads to a slope of 1.10 ($R^2 = 0.54$), but still a high intercept of 11.4. This might be due to the uncertainties of the varying ZAMS calibration factors (RIE, NO_2/NO ratio of pure inorganic nitrate, *etc.*) and the above-mentioned temporal and spatial variance of the LVOOA factor. Reasonably, also the slope of the regression line from $n_{e_{NH_4}}$ *versus* the summed molar CO_2^+ concentrations from both SOA factors acquired by the ToF-AMS for its entire campaign is lower (0.80) than the one shown in Fig. 7a, but the regression has a better coefficient of $R^2 = 0.70$.

Conclusion

We show that in NH_3 rich environments like the Netherlands, NH_3 uptake by acidic organic aerosol increases the total aerosol mass. As demonstrated by the Zeppelin flights, excess ammonium is a regional phenomenon, extending several 100 m in height into the planetary boundary layer. It has been previously suggested that reduction of ammonia emissions would enhance the mitigation of aerosol mass regionally due to the reduction of ammonium nitrate or ammonium sulphate in addition to effects achievable by reducing SO_2 and NO_x emissions alone (ref. 71 for Europe and ref. 72 for southwestern United States). We suggest that an additional benefit in reduced NH_3 emission can be achieved, as this should also reduce the formation of particulate organic ammonium salts.

Ammonia sources are typically associated with agricultural sources. Through the development and widespread application of selective catalytic reduction (SCR) converters to reduce NO_x emissions from fuel combustion, traffic is becoming an increasingly important source of NH_3.[3,4] This includes emissions from ships, diesel locomotives, or gas turbines, and of increasing importance are those from heavy-duty vehicles and passenger cars using diesel engines.[73] The findings of this work emphasize the need for control measures for traffic emission of NH_3, to reduce effects on aerosol mass through organic ammonium salt formation.

Furthermore, the uptake of NH_3 on organics as investigated in this work may alter important aerosol characteristics by enhancing the life time of aerosol due to low vapor pressures of the formed salts[74] and could change hygroscopic[23] and optical properties[24] thus impacting on the climate effects of aerosol.

Acknowledgements

References

1 K. W. Van der Hoek, *Atmos. Environ.*, 1998, **32**, 315–316.

2 B. Rumburg, G. H. Mount, D. Yonge, B. Lamb, H. Westberg, J. Filipy, J. Bays, R. Kincaid and K. Johnson, *Atmos. Environ.*, 2006, **40**, 7246–7258.

3 R. Matsumoto, N. Umezawa, M. Karaushi, S.-I. Yonemochi and K. Sakamoto, *Water, Air, Soil Pollut.*, 2006, **173**, 355–371.

4 J. Zheng, Y. Ma, M. Chen, Q. Zhang, L. Wang, A. F. Khalizov, L. Yao, Z. Wang, X. Wang and L. Chen, *Atmos. Environ.*, 2015, **102**, 249–259.

5 P. S. Monks, C. Granier, S. Fuzzi, A. Stohl, M. L. Williams, H. Akimoto, M. Amann, A. Baklanov, U. Baltensperger, I. Bey, N. Blake, R. S. Blake, K. Carslaw, O. R. Cooper, F. Dentener, D. Fowler, E. Fragkou, G. J. Frost, S. Generoso, P. Ginoux, V. Grewe, A. Guenther, H. C. Hansson, S. Henne, J. Hjorth, A. Hofzumahaus, H. Huntrieser, I. S. A. Isaksen, M. E. Jenkin, J. Kaiser, M. Kanakidou, Z. Klimont, M. Kulmala, P. Laj, M. G. Lawrence, J. D. Lee, C. Liousse, M. Maione, G. McFiggans, A. Metzger, A. Mieville, N. Moussiopoulos, J. J. Orlando, C. D. O'Dowd, P. I. Palmer, D. D. Parrish, A. Petzold, U. Platt, U. Pöschl, A. S. H. Prevot, C. E. Reeves, S. Reimann, Y. Rudich, K. Sellegri, R. Steinbrecher, D. Simpson, H. Ten Brink, J. Theloke, G. R. Van der Werf, R. Vautard, V. Vestreng, C. Vlachokostas and R. von Glasow, *Atmos. Environ.*, 2009, **43**, 5268–5350.

6 V. Vestreng, G. Myhre, H. Fagerli, S. Reis and L. Tarrason, *Atmos. Chem. Phys.*, 2007, **7**, 3663–3681.

7 M. Schaap, R. P. Otjes and E. P. Weijers, *Atmos. Chem. Phys.*, 2011, **11**, 11041–11053.

8 M. Kulmala, A. Asmi, H. K. Lappalainen, U. Baltensperger, J.-L. Brenguier, M. C. Facchini, H.-C. Hansson, O. Hov, C. D. O'Dowd, U. Pöschl, A. Wiedensohler, R. Boers, O. Boucher, G. De Leeuw, H. A. C. Denier van der Gon, J. Feichter, R. Krejci, P. Laj, H. Lihavainen, U. Lohmann, G. McFiggans, T. Mentel, C. Pilinis, I. Riipinen, M. Schulz, A. Stohl, E. Swietlicki, E. Vignati, C. Alves, M. Amann, M. Ammann, S. Arabas, P. Artaxo, H. Baars, D. C. S. Beddows, R. Bergstroem, J. P. Beukes, M. Bilde, J. F. Burkhart, F. Canonaco, S. L. Clegg, H. Coe, S. Crumeyrolle, B. D'Anna, S. Decesari, S. Gilardoni, M. Fischer, A. M. Fjaeraa, C. Fountoukis, C. George, L. Gomes, P. Halloran, T. Hamburger, R. M. Harrison, H. Herrmann, T. Hoffmann, C. Hoose, M. Hu, A. Hyvärinen, U. Horrak, Y. Iinuma, T. Iversen, M. Josipovic, M. Kanakidou, A. Kiendler-Scharr, A. Kirkevag, G. Kiss, Z. Klimont, P. Kolmonen, M. Komppula, J.-E. Kristjaensson, L. Laakso, A. Laaksonen, L. Labonnote, V. A. Lanz, K. E. J. Lehtinen, L. V. Rizzo,

R. Makkonen, H. E. Manninen, G. McMeeking, J. Merikanto, A. Minikin, S. Mirme, W. T. Morgan, E. Nemitz, D. O'Donnell, T. S. Panwar, H. Pawlowska, A. Petzold, J. J. Pienaar, C. Pio, C. Plass-Duelmer, A. S. H. Prevot, S. Pryor, C. L. Reddington, G. Roberts, D. Rosenfeld, J. Schwarz, O. Seland, K. Sellegri, X. J. Shen, M. Shiraiwa, H. Siebert, B. Sierau, D. Simpson, J. Y. Sun, D. Topping, P. Tunved, P. Vaattovaara, V. Vakkari, J. P. Veefkind, A. Visschedijk, H. Vuollekoski, R. Vuolo, B. Wehner, J. Wildt, S. Woodward, D. R. Worsnop, G.-J. van Zadelhoff, A. A. Zardini, K. Zhang, P. G. van Zyl, V.-M. Kerminen, K. S Carslaw and S. N. Pandis, *Atmos. Chem. Phys.*, 2011, **11**, 13061–13143.

9 V.-M. Kerminen, C. Ojanen, T. Pakkanen, R. Hillamo, M. Aurela and J. Meriläinen, *J. Aerosol Sci.*, 2000, **31**, 349–362.

10 A. Limbeck and H. Puxbaum, *Atmos. Environ.*, 1999, **33**, 1847–1852.

11 A. Röhrl and G. Lammel, *Environ. Sci. Technol.*, 2001, **35**, 95–101.

12 R. Sempére and K. Kawamura, *Atmos. Environ.*, 1994, **28**, 449–459.

13 G. Wang, S. Niu, C. Liu and L. Wang, *Atmos. Environ.*, 2002, **36**, 1941–1950.

14 X. Yao, M. Fang, C. K. Chan, K. F. Ho and S. C. Lee, *Atmos. Environ.*, 2004, **38**, 963–970.

15 M. Mochida, K. Kawamura, N. Umemoto, M. Kobayashi, S. Matsunaga, H.-J. Lim, B. J. Turpin, T. S. Bates and B. R. T. Simoneit, *J. Geophys. Res.: Atmos.*, 2003, **108**(D23), 8638.

16 H. Wang, K. Kawamura and K. Yamazaki, *J. Atmos. Chem.*, 2006, **53**, 43–61.

17 A. A. Mensah, PhD thesis, Universität zu Köln, 2011.

18 A. L. Paciga, I. Riipinen and S. N. Pandis, *Environ. Sci. Technol.*, 2014, **48**, 13769–13775.

19 S. Metzger, N. Mihalopoulos and J. Lelieveld, *Atmos. Chem. Phys.*, 2006, **6**, 2549–2567.

20 M. Mircea, M. C. Facchini, S. Decesari, F. Cavalli, L. Emblico, S. Fuzzi, A. Vestin, J. Rissler, E. Swietlicki, G. Frank, M. O. Andreae, W. Maenhaut, Y. Rudich and P. Artaxo, *Atmos. Chem. Phys.*, 2005, **5**, 3111–3126.

21 I. Trebs, S. Metzger, F. X. Meixner, G. Helas, A. Hoffer, Y. Rudich, A. H. Falkovich, M. A. L. Moura, R. S. Da Silva, P. Artaxo, J. Slanina and M. O. Andreae, *J. Geophys. Res.: Atmos.*, 2005, **110**(D7), D07303.

22 R. W. Pinder, P. J. Adams and S. N. Pandis, *Environ. Sci. Technol.*, 2007, **41**, 380–386.

23 E. Dinar, T. Anttila and Y. Rudich, *Environ. Sci. Technol.*, 2008, **42**, 793–799.

24 A. Laskin, J. Laskin and S. A. Nizkorodov, *Chem. Rev.*, 2015, **115**, 4335–4382.

25 A. T. Vermeulen, A. Hensen, M. E. Popa, W. C. M. Van den Bulk and P. A. C. Jongejan, *Atmos. Meas. Tech.*, 2011, **4**, 617–644.

26 P. Schlag, A. Kiendler-Scharr, M. J. Blom, F. Canonaco, J. S. Henzing, M. Moerman, A. S. H. Prévôt and R. Holzinger, *Atmos. Chem. Phys.*, 2016, **16**, 8831–8847.

27 A. A. Mensah, R. Holzinger, R. Otjes, A. Trimborn, T. F. Mentel, H. Ten Brink, B. Henzing and A. Kiendler-Scharr, *Atmos. Chem. Phys.*, 2012, **12**, 4723–4742.

28 H. Russchenberg, F. Bosveld, D. Swart, H. Ten Brink, G. De Leeuw, R. Uijlenhoet, B. Arbesser-Rastburg, H. van der Marel, L. Ligthart, R. Boers and A. Apituley, *IEICE T Commun*, 2005, **E88B**, 2252–2258.

29 A. P. Ulden and J. Wieringa, *Boundary-Layer Meteorology*, 1996, **78**, 39–69.

30 P. F. DeCarlo, J. R. Kimmel, A. Trimborn, M. J. Northway, J. T. Jayne, A. C. Aiken, M. Gonin, K. Fuhrer, T. Horvath, K. S. Docherty, D. R. Worsnop and J. L. Jimenez, *Anal. Chem.*, 2006, **78**, 8281–8289.

31 J. T. Jayne, D. C. Leard, X. F. Zhang, P. Davidovits, K. A. Smith, C. E. Kolb and D. R. Worsnop, *Aerosol Sci. Technol.*, 2000, **33**, 49–70.

32 J. L. Jimenez, J. T. Jayne, Q. Shi, C. E. Kolb, D. R. Worsnop, I. Yourshaw, J. H. Seinfeld, R. C. Flagan, X. Zhang, K. A. Smith, J. W. Morris and P. Davidovits, *J. Geophys. Res.: Atmos.*, 2003, **108**(D7), 8425.

33 S. M. Pieber, I. El Haddad, J. G. Slowik, M. R. Canagaratna, J. T. Jayne, S. M. Platt, C. Bozzetti, K. R. Daellenbach, R. Fröhlich, A. Vlachou, F. Klein, J. Dommen, B. Miljevic, J. L. Jiménez, D. R. Worsnop, U. Baltensperger and A. S. H. Prévôt, *Environ. Sci. Technol.*, 2016, **50**, 10494–10503.

34 T. C. Bond, S. J. Doherty, D. W. Fahey, P. M. Forster, T. Berntsen, B. J. DeAngelo, M. G. Flanner, S. Ghan, B. Kärcher, D. Koch, S. Kinne, Y. Kondo, P. K. Quinn, M. C. Sarofim, M. G. Schultz, M. Schulz, C. Venkataraman, H. Zhang, S. Zhang, N. Bellouin, S. K. Guttikunda, P. K. Hopke, M. Z. Jacobson, J. W. Kaiser, Z. Klimont, U. Lohmann, J. P. Schwarz, D. Shindell, T. Storelvmo, S. G. Warren and C. S. Zender, *J. Geophys. Res.: Atmos.*, 2013, **118**, 5380–5552.

35 F. Rubach, PhD thesis, Bergische Universität Wuppertal, 2013.

36 X. Li, F. Rohrer, A. Hofzumahaus, T. Brauers, R. Häseler, B. Bohn, S. Broch, H. Fuchs, S. Gomm, F. Holland, J. Jäger, J. Kaiser, F. N. Keutsch, I. Lohse, K. Lu, R. Tillmann, R. Wegener, G. M. Wolfe, T. F. Mentel, A. Kiendler-Scharr and A. Wahner, *Science*, 2014, **344**, 292–296.

37 B. Rosati, M. Gysel, F. Rubach, T. F. Mentel, B. Goger, L. Poulain, P. Schlag, P. Miettinen, A. Pajunoja, A. Virtanen, H. Klein Baltink, J. S. B. Henzing, J. Größ, G. P. Gobbi, A. Wiedensohler, A. Kiendler-Scharr, S. Decesari, M. C. Facchini, E. Weingartner and U. Baltensperger, *Atmos. Chem. Phys.*, 2016, **16**, 7295–7315.

38 J. Jäger, Dissertation, Universität zu Köln, 2014.

39 R. Bahreini, E. J. Dunlea, B. M. Matthew, C. Simons, K. S. Docherty, P. F. DeCarlo, J. L. Jimenez, C. A. Brock and A. M. Middlebrook, *Aerosol Sci. Technol.*, 2008, **42**, 465–471.

40 A. M. Middlebrook, R. Bahreini, J. L. Jimenez and M. R. Canagaratna, *Aerosol Sci. Technol.*, 2012, **46**, 258–271.

41 F. Drewnick, S. S. Hings, P. DeCarlo, J. T. Jayne, M. Gonin, K. Fuhrer, S. Weimer, J. L. Jimenez, K. L. Demerjian, S. Borrmann and D. R. Worsnop, *Aerosol Sci. Technol.*, 2005, **39**, 637–658.

42 M. R. Alfarra, H. Coe, J. D. Allan, K. N. Bower, H. Boudries, M. R. Canagaratna, J. L. Jimenez, J. T. Jayne, A. A. Garforth, S.-M. Li and D. R. Worsnop, *Atmos. Environ.*, 2004, **38**, 5745–5758.

43 M. R. Canagaratna, J. T. Jayne, J. L. Jimenez, J. D. Allan, M. R. Alfarra, Q. Zhang, T. B. Onasch, F. Drewnick, H. Coe, A. Middlebrook, A. Delia, L. R. Williams, A. M. Trimborn, M. J. Northway, P. F. DeCarlo, C. E. Kolb, P. Davidovits and D. R. Worsnop, *Mass Spectrom. Rev.*, 2007, **26**, 185–222.

44 A. C. Aiken, P. F. DeCarlo and J. L. Jimenez, *Anal. Chem.*, 2007, **79**, 8350–8358.

45 A. C. Aiken, P. F. DeCarlo, J. H. Kroll, D. R. Worsnop, J. A. Huffman, K. S. Docherty, I. M. Ulbrich, C. Mohr, J. R. Kimmel, D. Sueper, Y. Sun, Q. Zhang, A. Trimborn, M. Northway, P. J. Ziemann, M. R. Canagaratna,

T. B. Onasch, M. R. Alfarra, A. S. H. Prevot, J. Dommen, J. Duplissy, A. Metzger, U. Baltensperger and J. L. Jimenez, *Environ. Sci. Technol.*, 2008, **42**, 4478–4485.

46 M. R. Canagaratna, J. L. Jimenez, J. H. Kroll, Q. Chen, S. H. Kessler, P. Massoli, L. Hildebrandt Ruiz, E. Fortner, L. R. Williams, K. R. Wilson, J. D. Surratt, N. M. Donahue, J. T. Jayne and D. R. Worsnop, *Atmos. Chem. Phys.*, 2015, **15**, 253–272.

47 P. Paatero, *Chemom. Intell. Lab. Syst.*, 1997, **37**, 23–35.

48 P. Paatero and U. Tapper, *Environmetrics*, 1994, **5**, 111–126.

49 I. M. Ulbrich, M. R. Canagaratna, Q. Zhang, D. R. Worsnop and J. L. Jimenez, *Atmos. Chem. Phys.*, 2009, **9**, 2891–2918.

50 Q. Zhang, J. L. Jimenez, M. R. Canagaratna, I. M. Ulbrich, N. L. Ng, D. R. Worsnop and Y. Sun, *Anal. Bioanal. Chem.*, 2011, **401**, 3045–3067.

51 P. Paatero, *J. Comp. Graph. Stat.*, 1999, **8**, 854–888.

52 F. Canonaco, M. Crippa, J. G. Slowik, U. Baltensperger and A. S. H. Prevot, *Atmos Meas Tech*, 2013, **6**, 3649–3661.

53 P. Paatero and P. K. Hopke, *Anal. Chim. Acta*, 2003, **490**, 277–289.

54 C. J. Hennigan, J. Izumi, A. P. Sullivan, R. J. Weber and A. Nenes, *Atmos. Chem. Phys.*, 2015, **15**, 2775–2790.

55 I. Trebs, F. X. Meixner, J. Slanina, R. Otjes, P. Jongejan and M. O. Andreae, *Atmos. Chem. Phys.*, 2004, **4**, 967–987.

56 D. K. Farmer, A. Matsunaga, K. S. Docherty, J. D. Surratt, J. H. Seinfeld, P. J. Ziemann and J. L. Jimenez, *Proc. Natl. Acad. Sci. U. S. A.*, 2010, **107**, 6670–6675.

57 A. Kiendler-Scharr, A. A. Mensah, E. Friese, D. Topping, E. Nemitz, A. S. H. Prevot, M. Äijälä, J. Allan, F. Canonaco, M. Canagaratna, S. Carbone, M. Crippa, M. Dall Osto, D. A. Day, P. De Carlo, C. F. Di Marco, H. Elbern, A. Eriksson, E. Freney, L. Hao, H. Herrmann, L. Hildebrandt, R. Hillamo, J. L. Jimenez, A. Laaksonen, G. McFiggans, C. Mohr, C. O'Dowd, R. Otjes, J. Ovadnevaite, S. N. Pandis, L. Poulain, P. Schlag, K. Sellegri, E. Swietlicki, P. Tiitta, A. Vermeulen, A. Wahner, D. Worsnop and H. C. Wu, *Geophys. Res. Lett.*, 2016, **43**, 7735–7744.

58 M. Crippa, F. Canonaco, V. A. Lanz, M. Äijälä, J. D. Allan, S. Carbone, G. Capes, D. Ceburnis, M. Dall'Osto, D. A. Day, P. F. DeCarlo, M. Ehn, A. Eriksson, E. Freney, L. Hildebrandt Ruiz, R. Hillamo, J. L. Jimenez, H. Junninen, A. Kiendler-Scharr, A.-M. Kortelainen, M. Kulmala, A. Laaksonen, A. A. Mensah, C. Mohr, E. Nemitz, C. O'Dowd, J. Ovadnevaite, S. N. Pandis, T. Petäjä, L. Poulain, S. Saarikoski, K. Sellegri, E. Swietlicki, P. Tiitta, D. R. Worsnop, U. Baltensperger and A. S. H. Prevot, *Atmos. Chem. Phys.*, 2014, **14**, 6159–6176.

59 J. Schmale, J. Schneider, E. Nemitz, Y. S. Tang, U. Dragosits, T. D. Blackall, P. N. Trathan, G. J. Phillips, M. Sutton and C. F. Braban, *Atmos. Chem. Phys.*, 2013, **13**, 8669–8694.

60 S. R. Zorn, F. Drewnick, M. Schott, T. Hoffmann and S. Borrmann, *Atmos. Chem. Phys.*, 2008, **8**, 4711–4728.

61 M. Crippa, I. El Haddad, J. G. Slowik, P. F. DeCarlo, C. Mohr, M. F. Heringa, R. Chirico, N. Marchand, J. Sciare, U. Baltensperger and A. S. H. Prevot, *J. Geophys. Res.: Atmos.*, 2013, **118**, 1950–1963.

62 A. A. Mensah, A. Buchholz, T. F. Mentel, R. Tillmann and A. Kiendler-Scharr, *J. Aerosol Sci.*, 2011, **42**, 11–19.

63 M. Paglione, A. Kiendler-Scharr, A. A. Mensah, E. Finessi, L. Giulianelli, S. Sandrini, M. C. Facchini, S. Fuzzi, P. Schlag, A. Piazzalunga, E. Tagliavini, J. S. Henzing and S. Decesari, *Atmos. Chem. Phys.*, 2014, **14**, 25–45.

64 S. Zhou, S. Collier, J. Xu, F. Mei, J. Wang, Y.-N. Lee, A. J. Sedlacek, S. R. Springston, Y. Sun and Q. Zhang, *J. Geophys. Res.: Atmos.*, 2016, **121**, 6049–6065.

65 Y. B. Lim, Y. Tan, M. J. Perri, S. P. Seitzinger and B. J. Turpin, *Atmos. Chem. Phys.*, 2010, **10**, 10521–10539.

66 M. Z. H. Rozaini, in *Atmospheric Aerosols – Regional Characteristics – Chemistry and Physics*, InTech, Rijeka, 2012, DOI: 10.5772/50127.

67 P. Schlag, Dissertation, Universität zu Köln, 2015.

68 J. Duplissy, P. F. DeCarlo, J. Dommen, M. R. Alfarra, A. Metzger, I. Barmpadimos, A. S. H. Prevot, E. Weingartner, T. Tritscher, M. Gysel, A. C. Aiken, J. L. Jimenez, M. R. Canagaratna, D. R. Worsnop, D. R. Collins, J. Tomlinson and U. Baltensperger, *Atmos. Chem. Phys.*, 2011, **11**, 1155–1165.

69 R. G. Bates and G. D. Pinching, *J. Am. Chem. Soc.*, 1950, **72**, 1393–1396.

70 E. R. Graber and Y. Rudich, *Atmos. Chem. Phys.*, 2006, **6**, 729–753.

71 A. G. Megaritis, C. Fountoukis and S. N. Pandis, in *Air Pollution Modeling and its Application XXII*, ed. D. G. Steyn, P. J. H. Builtjes and R. M. A. Timmermans, Springer Netherlands, 2014, ch. 56, pp. 333–338, DOI: 10.1007/978-94-007-5577-2_56.

72 Y. Zhang and S.-Y. Wu, *Aerosol Air Qual. Res.*, 2013, **13**, 1475–1491.

73 P. Forzatti, I. Nova and E. Tronconi, *Angew. Chem.*, 2009, **121**, 8516–8518.

74 S. A. K. Häkkinen, V. F. McNeill and I. Riipinen, *Environ. Sci. Technol.*, 2014, **48**, 13718–13726.